UCLA
UCLA Previously Published Works

Title

Anatomic localization of O6-methylguanine DNA methyltransferase (MGMT) promoter methylated and unmethylated tumors: A radiographic study in 358 de novo human glioblastomas

Permalink

https://escholarship.org/uc/item/8sd5t9nj

Journal

NeuroImage, 59(2)

ISSN

1053-8119

Authors

Ellingson, Benjamin M
Cloughesy, Timothy F
Pope, Whitney B
et al.

Publication Date

2012

DOI

10.1016/j.neuroimage.2011.09.076

Peer reviewed

eScholarship.org Powered by the California Digital Library
University of California

NeuroImage 59 (2012) 908–916

Contents lists available at SciVerse ScienceDirect

NeuroImage

journal homepage: www.elsevier.com/locate/ynimg

Anatomic localization of O6-methylguanine DNA methyltransferase (MGMT) promoter methylated and unmethylated tumors: A radiographic study in 358 de novo human glioblastomas ☆

Benjamin M. Ellingson [a,*], Timothy F. Cloughesy [b], Whitney B. Pope [a], Taryar M. Zaw [a], Heidi Phillips [c], Shadi Lalezari [b], Phioanh L. Nghiemphu [b], Hassana Ibrahim [a], Kourosh M. Naeini [a], Robert J. Harris [a], Albert Lai [b]

[a] Department of Radiological Sciences, David Geffen School of Medicine, University of California Los Angeles, Los Angeles, CA 90095, USA
[b] Department of Neurology, David Geffen School of Medicine, University of California Los Angeles, Los Angeles, CA 90095, USA
[c] Department of Tumor Biology and Angiogenesis, Genentech, Inc., San Francisco, CA 94080, USA

ARTICLE INFO

Article history:
Received 13 July 2011
Revised 27 September 2011
Accepted 29 September 2011
Available online 7 October 2011

Keywords:
Radiogenomics
MGMT
Glioblastoma
GBM
Tumor location

ABSTRACT

Promoter methylation of O6-methylguanine DNA methyltransferase (MGMT) is associated with a favorable prognosis in glioblastoma multiforme (GBM) and has been hypothesized to occur early in tumor transformation of glial cells. Thus, a possible link exists between the site of malignant transformation and MGMT promoter methylation status. Using the Analysis of Differential Involvement (ADIFFI) statistical mapping technique in a total of 358 patients with GBM, we demonstrate that human de novo GBMs occur in a high frequency contiguous with the posterior subventricular zone (SVZ); MGMT promoter methylated GBMs are lateralized to the left hemisphere, while MGMT unmethylated GBMs are lateralized to the right hemisphere; and tumors near the left temporal lobe have a significantly longer overall survival compared with tumors occurring elsewhere, independent of treatment or MGMT methylation status.

© 2011 Elsevier Inc. All rights reserved.

Introduction

Glioblastoma multiforme (GBM) is the most common, and unfortunately also the most lethal primary brain neoplasm. Despite advances in surgery, radiation and drug therapy, the median survival remains relatively unchanged and ranges from 12 to 15 months (Stupp et al., 2005). Although long-term survival is almost universally poor, a handful of prognostic factors have been identified that confer modest difference in survivability. These prognostic factors include age, performance and neurological status, extent of surgical resection, degree of necrosis and enhancement on preoperative magnetic resonance (MR) imaging, adjuvant therapy received, and tumor location (Fontaine and Paquis, 2010; Gorlia et al., 2008; Lacroix et al., 2001).

Although controversial, previous studies support tumor location as playing a role in prognosis (Fontaine and Paquis, 2010; Simpson et al., 1993), likely due to the genetic profile of tumor precursor cells and the stage in the development cycle that these cells transform (i.e. the glioma "cell of origin") (Sanai et al., 2005). For example, an association between brain tumor location, growth pattern and tumor genetic signature has been shown with oligodendroliomas (Zlatescu et al., 2001). As explained in this study, different types of oligodendrogliomas may arise from different precursor cells that are relatively region-specific at inception or during brain development. In support of this hypothesis, germinal regions containing neural stem cells, including the subventricular zone (SVZ), have been proposed as a source for human gliomas (Globus and Kuhlenbeck, 1942). Also consistent with the hypothesis that tumor location reflects the contributions of specific precursor cells is the observation that medulloblastoma arises through abnormalities along a particular developmental pathway in a distinct population of progenitor cells (Marino et al., 2000; Pietsch et al., 1997). Additional evidence of isocitrate dehydrogenase 1 (IDH1) tumors originating from a distinct cell of origin giving rise to their predominant localization within the frontal lobe regions (Lai et al., in press) also supports this theory.

Abbreviations: GBM, glioblastoma multiforme; MGMT, O6-methylguanine DNA methyltransferase; SVZ, subventricular zone; ADIFFI, Analysis of Differential Involvement; MR/MRI, magnetic resonance imaging; IDH1, isocitrate dehydrogenase 1; TMZ, temozolomide; MSP, methylation-specific PCR.

☆ Grant support: UCLA Institute for Molecular Medicine Seed Grant (BME); UCLA Radiology Exploratory Research Grant (BME); Art of the Brain (TFC); Ziering Family Foundation in memory of Sigi Ziering (TFC); Singleton Family Foundation (TFC); Clarence Klein Fund for Neuro-Oncology (TFC).

* Corresponding author at: Department of Radiological Sciences, David Geffen School of Medicine, University of California Los Angeles, 924 Westwood Blvd., Suite 615, Los Angeles, CA 90024. Fax: +1 310 794 8657.
E-mail address: bellingson@mednet.ucla.edu (B.M. Ellingson).

1053-8119/$ – see front matter © 2011 Elsevier Inc. All rights reserved.
doi:10.1016/j.neuroimage.2011.09.076

MGMT promoter methylation and tumor localization

O6-methylguanine DNA methyltransferase (MGMT) promoter methylation is a favorable prognostic factor in patients treated with temozolomide (TMZ), a chemotherapeutic agent shown to prolong survival in patients with GBM (Stupp et al., 2005). The MGMT gene is located on chromosome 10q26 and encodes a DNA-repair protein, which removes alkyl groups from the O6 position of guanine. This is thought to be the same alkylation target of TMZ that triggers cytotoxicity. The MGMT gene is silenced by the methylation of its promoter, resulting in loss of MGMT expression and subsequently decreased DNA-repair activity. In other words, tumors with methylated MGMT promoter are more sensitive to TMZ treatment. These findings underscore the importance of MGMT promoter methylation status in prognosis and therapeutic guidance.

Topographic distribution of MGMT promoter methylated tumors is consistent with the hypothesis of a distinct "cell of origin". Specifically, MGMT promoter methylation is thought to occur as part of a genetic signature that develops from lower-grade gliomas (Eoli et al., 2007), and this transformation is thought to occur early in tumor development within glial cells predestined for specific locations (Drabycz et al., 2010). This appears plausible, especially in light of evidence supporting GBM development from neural stem cells (Nicolis, 2007) and the fact many gliomas are contiguous with the SVZ (Alvarez-Buylla and Garcia-Verdugo, 2002), known to harbor neural stem cells. Two recent studies examined the relationship between MGMT promoter methylation status and tumor location, but arrived at different conclusions. In a 2007 study by Eoli et al. (Eoli et al., 2007), MGMT promoter methylated tumors were found to occur more often in parietal and occipital lobes, whereas tumors without MGMT promoter methylation were more often in the temporal lobes. In a recent publication by Drabycz et al., (2010), no significant difference between the locations of MGMT methylated and unmethylated GBM tumors was found. Both these studies, however, were limited by relatively small sample sizes ($n=86$, 45 methylated, 41 unmethylated; and $n=72$, 36 methylated, 36 unmethylated patients, respectively).

Despite noting a general higher frequency in different regions of the brain, no tools have been developed for voxel-wise statistical comparison for testing tumor localization. The current study involves a new technique called Analysis of Differential Involvement (ADIFFI) maps and applies this technique to MGMT promoter methylated versus non-methylated tumors in order to determine whether these tumors are localized to a particular area of the brain more often than chance. In addition, the current study examined 358 patients, representing the largest and most comprehensive study examining radiological difference between MGMT methylated versus non-methylated GBMs.

Methods

Patients

All patients participating in this study signed institutional review board-approved informed consent to have their data collected and stored in our institution's neuro-oncology database. Data acquisition and storage were performed in compliance with all applicable Health Insurance Portability and Accountability Act (HIPAA) regulations. The study spanned April 2000 through March 2011. A total of $n=358$ patients with de novo GBM were enrolled in this retrospective study who met the following criteria: 1) pathology confirmed GBM with no previous history of primary CNS tumors, 2) pre-surgical T2/FLAIR images and/or post-contrast T1-weighted images, and 3) tissue available for testing MGMT promoter methylation status. Additional patient characteristics are summarized in Table 1.

Table 1
Patient characteristics. T2/FLAIR = number of patients with adequate T2-weighted or fluid-attenuated inversion recovery (FLAIR) images. T1 + C = number of patients with adequate post-contrast T1-weighted images. KPS = Karnofsky Performance Status. * = Standard Deviation.

Total	*358*
T2/FLAIR	*353*
Methylated	*128*
Unmethylated	*225*
T1 + C	*323*
Methylated	*123*
Unmethylated	*200*
Gender	
Male	*222*
Female	*136*
Age	*56.4 ± 10.2**
KPS	*72.4 ± 10.1**

MGMT methylation analysis

MGMT methylation analysis was performed by methylation-specific PCR (MSP) according to a previously published protocol (Hegi et al., 2005) with some slight modifications as described in another publication (Lai et al., 2010). To generate bisulfite modified DNA, genomic DNA isolated from formalin fixed, paraffin-embedded tissue using Recoverall Total Nucleic Acid Isolation Kit (Ambion, Austin, TX) was modified using the EZ DNA Methylation-Gold Kit (ZymoResearch, Orange,CA) following the manufacturer's protocol. Samples were subjected to a two-stage nested PCR strategy using: first-stage primers (5′-GGATATGTTGGGATAGTT-3′ and 5′-CCAAAAACCCCAAACCC-3′) and second-stage primers (unmethylated reaction: 5′-TTTGTGTTTTGATGTTTGTAGGTTTTTGT-3′ and 5′-AACTCCACACTCTTCCAAAAACAAAACA-3′; methylated reaction: 5′-TTTCGACGTTCGTAGGTTTTCGC-3' and 5′-GCACTCTTCCGAAAACGAA-ACG-3′). PCR products were analyzed on 3% agarose gels. Positive and negative control samples for the MSP reaction were U87MG DNA treated with SssI methyltransferase (New England Biolabs, Ipswich, MA) and whole-genome amplification ofU87MGDNAusing the GenomiPhi V2 Amplification Kit (Amersham Biosciences, Piscataway, NJ), respectively.

Magnetic Resonance Imaging

Data was collected on either a 1.5 T (GE LX Echospeed or GE HDx Excite; General Electric Medical Systems, Waukesha, WI; Siemens Avanto TIM Class or Siemens Sonata Maestro Class; Siemens Medical Solutions, Erlangen, Germany) or 3.0 T (Siemens Trio TIM Class or Siemens Allegra TIM Class; Siemens Medical Solutions, Erlangen Germany) using pulse sequences supplied by the scanner manufacturer. Standard anatomical MRI sequences consisted of axial T1 weighted, T2-weighted fast spin-echo, and fluid attenuated inversion recovery (FLAIR). Additionally, gadopentate dimeglumine (Gd-DTPA, Magnevist®; Berlex, Wayne, NJ; 0.1 mmol/kg) or gadobenate dimeglumine (Gd-BOPTA, Multihance®; Bracco S.p.A., Milano, Italy; 0.1 mmol/kg) enhanced axial and coronal T1-weighted images (i.e. post-contrast, contrast-enhanced, T1-weighted images). Axial images were used for ADIFFI analysis, which consisted of slices 3–5 mm thick and 0–1 mm interslice gap. Echo and repetition times (TE and TR) for MR acquisition differed from scanner to scanner according to field strength and our specific clinical protocols.

Image registration

All images for each patient were registered to a high-resolution (1.0 mm isotropic), T1-weighted brain atlas (MNI152; Montreal Neurological Institute) using a mutual information algorithm and a 12-degree of freedom transformation using FSL (FMRIB, Oxford, UK; http://www.fmrib.ox.ac.uk/fsl/). Fine registration (1–2 and 1–2 voxels) was then performed using a Fourier transform-based, 6 degree

of freedom, rigid body registration algorithm (Cox and Jesmanowicz, 1999) followed by visual inspection to ensure adequate alignment by two investigators (T.Z. and B.M.E.). Manual adjustment, if necessary, was performed using the *tkregister2* routine available from Freesurfer (surfer.nmr.mgh.harvard.edu; Massachusetts General Hospital — Harvard Medical School, Boston, MA).

Regions of Interest (ROIs)

After image registration, T2/FLAIR images and post-contrast T1-weighted images were segmented (Fig. 1A) using a semi-automated procedure consisting of 1) manually defining the relative region of tumor occurrence, 2) thresholding either the T2/FLAIR or post-contrast images within these regions using an empirical threshold combined with a region-growing algorithm, and then 3) manually editing the resulting masks to exclude any obvious errors in segmentation. Regions of central necrosis (hypointense regions on T1-weighted images) were included in the study to outline the entire extent of the tumor. Note that tumor volume calculations (T2/FLAIR and contrast-enhancing) were calculated with respect to pre-registered tumor resolution and locations by taking into consideration the affine transformation matrix. Regions containing both vasogenic edema and infiltrating tumor were included in T2/FLAIR ROIs due to the known difficulty separating these tissues. All but five patients had T2/FLAIR images available (353/358, or 99%) and all but five patients who had post-contrast T1-weighted images also had T2/FLAIR images available (323/353, or 92%). Although T2/FLAIR and post-contrast T1-weighted images were used for segmentation, it should be noted that the visual tumor really only reflects the "tip of the iceberg" with respect to the total underlying tumor burden (Harpold et al., 2007; Swanson et al., 2003).

Analysis of Differential Involvement (ADIFFI)

Analysis of differential involvement (ADIFFI) analysis consisted of implementing a two-tailed Fisher's exact test to evaluate a 2×2 contingency table comparing MGMT methylated versus unmethylated and tumor versus non-tumor for each image voxel, repeated once for T2/FLAIR ROIs and once for contrast-enhancing tumor ROIs (Fig. 1B). The use of Fisher's exact test on a voxel-wise basis has been implemented to study spatial regions of the brain involved in first-episode schizophrenia (Park et al., 2004) as well as to study localization of IDH1 mutant brain tumors (Lai et al., in press). This technique is similar to the voxel-based lesion-symptom mapping (VLSM) technique that has been used to map symptom locations in stroke patients (Bates et al., 2003). The 2×2 contingency table is shown in Fig. 1B and Table 2. According to Fisher's exact test, the probability of obtaining the observed "pattern" in the 2×2 contingency table is given by the hypergeometric distribution:

$$p = \frac{\binom{a+b}{a}\binom{c+d}{c}}{\binom{n}{a+c}} \quad (1)$$

which can be rewritten as

$$p = \frac{(a+b)!(c+d)!(a+c)!(b+d)!}{a!b!c!d!n!} \quad (2)$$

To calculate the significance of the observed pattern in the contingency table corresponding to the total probability of observing a pattern in the contingency table as extreme or more extreme, the *p*-

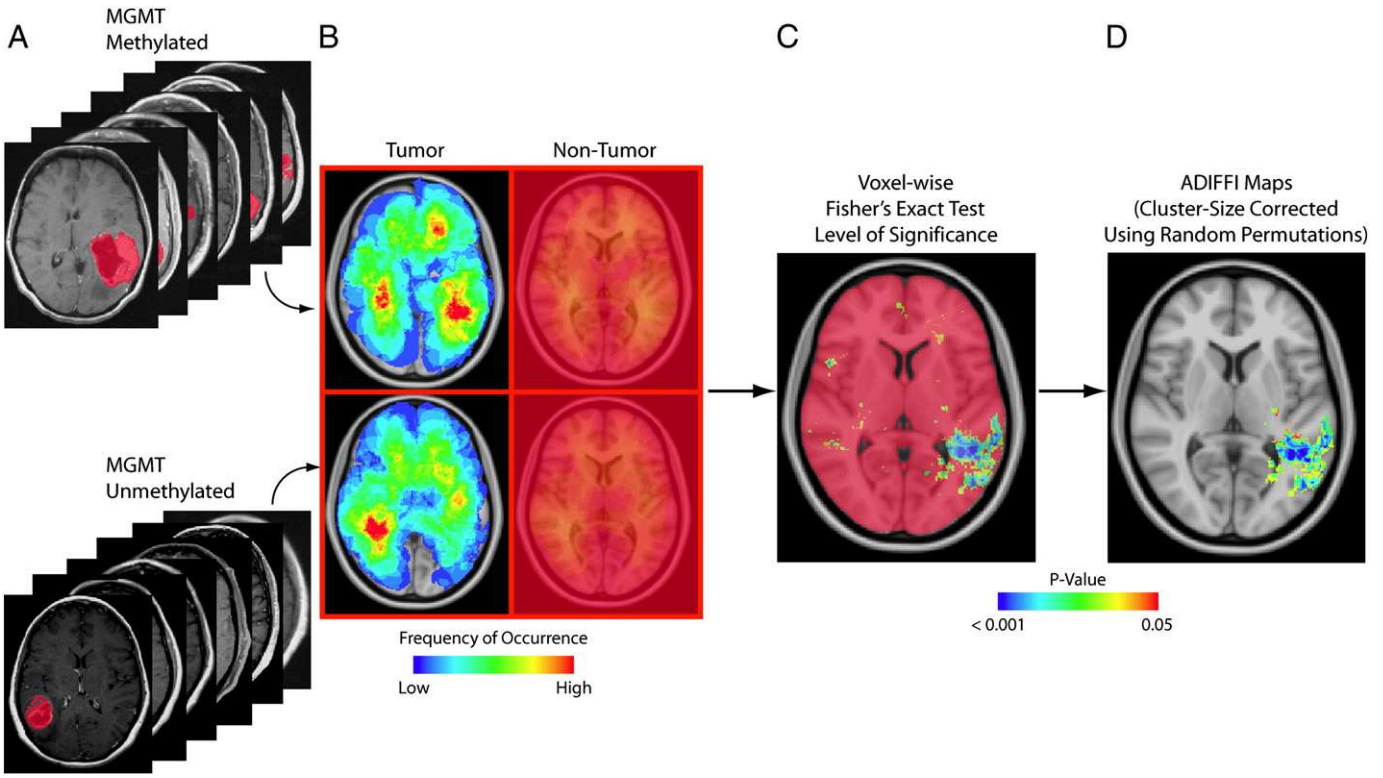

Fig. 1. Analysis of differential involvement (ADIFFI) statistical mapping methodology. First, all images were registered to a high-resolution T1-weighted MNI brain atlas. A) Next, contrast-enhancing and T2/FLAIR regions of interest were contoured for both MGMT promoter methylated and unmethylated tumors. B) All tumors for the methylated and unmethylated groups were combined into a 2×2 contingency table (see Table 2), where each voxel is classified as either methylated vs. unmethylated and tumor vs. non-tumor. C) Fisher's exact test was then performed on a voxel-wise basis throughout the brain. D) Lastly, permutation-based cluster-size correction was performed for statistically significant ($p < 0.05$) voxels to isolate cluster sizes that occur less than 5% by chance, resulting in the final ADIFFI maps.

Table 2
ADIFFI contingency table evaluated for each image voxel. a = number of MGMT methylated tumor occurring at the current voxel location; b = number of MGMT methylated tumors not occurring at the current voxel location; c = number of MGMT unmethylated tumors occurring at the current voxel location; d = number of MGMT unmethylated tumors not occurring at the current voxel location; a + b = total number of MGMT methylated tumors; c + d = total number of MGMT ummethylated tumors; a + c = total number of times tumor occurred at the current voxel location, regardless of MGMT status; b + d = total number of times tumor did not occur at the current voxel location, regardless of MGMT status; *n* = total number of tumors evaluated. Note: Independent contingency tables were created for T2/FLAIR and contrast-enhancing tumors.

	MGMT methylated	MGMT unmethylated	
Tumor	a	c	a + c
Non-tumor	b	d	b + d
	a + b	c + d	*n*

value for each voxel needs to be recalculated for all cases where the marginal totals are the same as the observed tables, and only cases where the arrangement is as extreme as the observed pattern. Then, for each iteration where values are incremented to calculate a more extreme pattern, the previous *p*-value in each image voxel is added to the current *p*-value until the most extreme pattern has been reached (which may vary from voxel to voxel). The final *p*-value represents the probability of observing the given pattern in the contingency table, or simply the probability that this pattern of tumor occurrence happened by chance (Fig. 1C). A parametric surface showing the relationship between the number of methylated and unmethylated tumors and resulting *p*-value is shown in Supplemental Fig. 1. For practical implementation purposes, only voxels containing at least one tumor occurrence for both methylated and unmethylated were analyzed.

Correction for cluster-size using random permutations

Multiple comparison corrections needed to be performed on the resulting statistical maps because as many as two million voxel-wise calculations were performed. Simple Bonferroni or false-discovery rate correction would likely be too conservative to produce any effect, and additionally we desired to isolate spatially distinct *clusters* associated with significant differences between MGMT promoter methylation status. In order to accomplish this we performed a cluster-based permutation correction, outlined by Bullmore et al. (Bullmore et al., 1999) (Fig. 1D), where tumors were first assigned randomly to each category, statistical testing was performed, and the size of statistically significant clusters were documented many times to determine how likely a specific cluster size would occur due to chance. More specifically, all T2/FLAIR tumors were uncategorized and reassigned randomly to either "methylated" or "unmethylated" groups according to the same proportions (e.g. for T2/FLAIR tumors, 141 were assigned to "methylated" and 238 were assigned to "unmethylated"). This process was permutated a total of 500 times for T2/FLAIR tumors, because these clusters were much larger than contrast-enhancing clusters, thus the resulting cluster-size threshold will be more conservative than the cluster-size threshold determined from contrast-enhancing clusters. ADIFFI analysis was then performed as outlined above after each permutation. Voxels showing $p < 0.05$ according to ADIFFI analyses were maintained and the images were clustered using the Analysis of Functional NeuroImaging toolkit (AFNI; afni.nimh.nih.gov/afni). All contiguous clusters greater than 2 voxels were stored, and cluster-size information was pooled across all 500 permutations similar to previous methods (Bullmore et al., 1999). Also, the largest cluster size was noted and used as a new independent variable.

Results from the permutation analysis suggest a probability density of all clusters resembled an exponential distribution (as noted elsewhere (Bullmore et al., 1999)), with a 5% chance of obtaining cluster sizes larger than 80 voxels for T2/FLAIR tumors (Supplemental Fig. 2A-B). When examining the largest cluster size as an independent variable, results after 500 permutations suggest the average maximum cluster size was approximately 5534 voxels with a standard deviation of 2767 voxels. Therefore, a cluster size threshold 12,335 voxels (or 12.3 cc) was used to ensure clusters larger than this threshold would occur in less than 5% of all random permutations. This cluster-size threshold (12.3 cc) resulted in two distinct clusters in T2/FLAIR tumors ("a" and "b" in Fig. 4A corresponding to a cluster volume of 234.2 cc and 14.7 cc, respectively) and a single cluster on contrast-enhancing tumors ("b" in Fig. 4B, corresponding to a cluster volume of 49.9 cc).

Survival analysis

Survival differences between MGMT promoter methylated and unmethylated patients were evaluated using log-rank survival analysis applied to Kaplan–Meier curves. Overall survival (OS) was defined from the time of initial tissue diagnosis until expiration. Additionally, survival differences between left and right hemispheric involvement were evaluated using log-rank statistical analysis applied to Kaplan–Meier curves. Patients having contrast-enhancing tumors confluent with the ADIFFI defined cluster in the left temporal lobe were evaluated using log-rank statistical analysis applied to Kaplan–Meier curves. To define this cluster, illustrated in "b" within Fig. 4B, a minimum cluster size of 20 cc of tissue was isolated in contiguous regions with *p*-value less than 0.05 on ADIFFI maps. Patients were stratified according to whether their contrast-enhancing tumor was connected to this cluster. Multivariate Cox proportional hazard analysis was performed to determine if age, Karnofsky performance status (KPS), MGMT methylation status, and tumors confluent with the ADIFFI cluster were significant predictors of OS.

Results

MGMT promoter methylated tumors have less T2/FLAIR hyperintense volume than unmethylated tumors

A significant difference in T2/FLAIR hyperintense volume was observed between MGMT methylated and unmethylated tumors (Fig. 2A, *t*-test, $p = 0.0092$); however, no difference in the volume of contrast-enhancement was detected (Fig. 2B, *t*-test, $p = 0.1381$). These results suggest MGMT promoter methylated tumors have less edema compared to MGMT unmethylated tumors.

T2/FLAIR hyperintense regions occur frequently in the posterior SVZ

Superimposing T2/FLAIR hyperintense regions of 353 GBM tumors into the same image space suggested a high number of GBMs have T2/FLAIR hyperintensity within the posterior aspect of the SVZ. Specifically, approximately 25% of all GBMs examined had T2/FLAIR hyperintensity near the left SVZ, while approximately 25% had T2/FLAIR hyperintensity near the right SVZ (Fig. 3A). Together, approximately 187 of 353 GBMs (approximately 50%) had T2/FLAIR hyperintensity near either the right or left SVZ. Contrast-enhancing regions were not localized to the posterior SVZ at such a high frequency (Fig. 3D), suggesting the higher frequency of T2/FLAIR hyperintensity localized to the posterior SVZ may be reflecting largely the presence of edema in these regions.

MGMT unmethylated tumors are lateralized to the right hemisphere

Qualitative examination of voxel-wise tumor probability maps suggest MGMT unmethylated tumors have T2/FLAIR hyperintensity lateralized to the right hemisphere (Fig. 3C). ADIFFI analysis (i.e. voxel-wise Fisher's exact test), after applying a permutation-based cluster-size correction (Bullmore et al., 1999), confirmed these

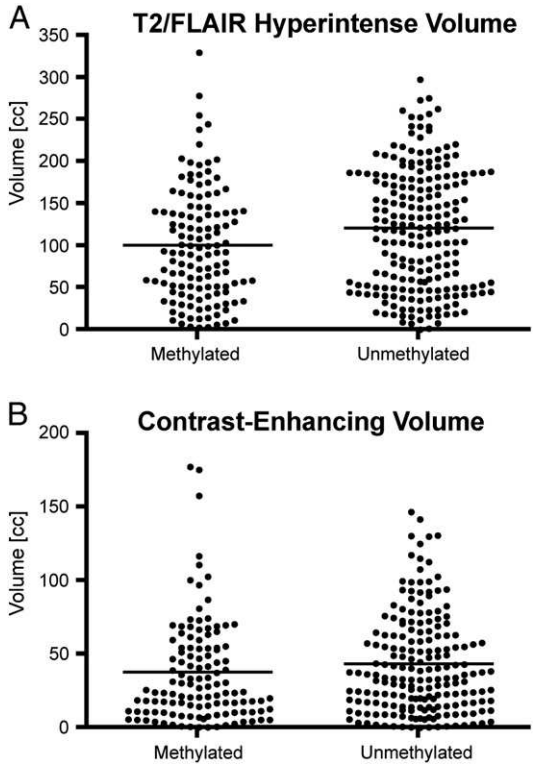

Fig. 2. Tumor volumes for A) T2/FLAIR hyperintense regions and B) contrast-enhancing volumes for MGMT promoter methylated and unmethylated patients. Results suggest a significantly higher volume of T2/FLAIR volumes in unmethylated tumors (*t*-test, $p = 0.0092$), but no difference in the volume of contrast-enhancing tumor (*t*-test, $p = 0.1381$).

qualitative observations (Fig. 3A), suggesting a low probability (low *p*-value) that the particular combination of tumor frequency between methylated and unmethylated tumors occurred by chance in the right hemisphere ("*a*" in Fig. 4A). Since either a large number of methylated or unmethylated tumors can cause a low *p*-value on ADIFFI maps, we examined the difference in tumor frequency between methylated and unmethylated tumors within regions exhibiting $p < 0.05$ on ADIFFI maps. Results suggest as many as 50 more unmethylated tumors occur on the right hemisphere compared with methylated tumors (Fig. 4A). In particular, regions of the right temporal lobe, right basal ganglia, and right SVZ demonstrated a significantly high frequency of tumor occurrence, implying that patients having T2/FLAIR hyperintensity on the right hemisphere are statistically more likely to have MGMT unmethylated tumors.

MGMT promoter methylated tumors are lateralized to the left hemisphere

Complementary to the findings in unmethylated tumors, examination of voxel-wise tumor probability maps suggest MGMT methylated tumors have *both* T2/FLAIR hyperintensity and contrast-enhancing regions lateralized to the left hemisphere (Figs. 3B, E). ADIFFI analysis after permutation-based cluster-size correction (Bullmore et al., 1999) confirmed that there was a low probability (low *p*-value) the particular combination of tumor frequency, as indicated by both T2/FLAIR hyperintensity ("*b*" in Fig. 4A) as well as contrast-enhancing regions ("*b*" in Fig. 4B), between methylated and unmethylated tumors occurred by chance in the left hemisphere. Interestingly, examination of the absolute difference in number of MGMT methylated versus unmethylated tumors within these regions on both ADIFFI maps generated from T2/FLAIR hyperintense regions ("*b*" in Fig. 4C) and contrast-enhancing regions ("*b*" in Fig. 4D) suggested MGMT promoter methylated tumors occurred more frequently in these regions. Specifically, regions proximal to the superior, middle, and inferior temporal gyrus, extending into white matter regions had a significantly high frequency of tumor occurrence, implying patients having contrast enhancing or T2/FLAIR hyperintense lesions in the left hemisphere near the temporal lobe are statistically more likely to have MGMT methylated tumors.

GBM patients with tumors touching ADIFFI-classified regions in left temporal lobe have significantly longer overall survival

As expected, overall survival (OS), regardless of extent of surgical resection or treatment, was significantly longer in GBM patients with MGMT promoter methylated tumors compared with unmethylated tumors (Fig. 5A; Log-rank, $p < 0.0001$). Surprisingly, GBM patients having contrast-enhancing tumors confluent with (connected to) the ADIFFI cluster defined in region "*b*" in Fig. 4 had a significantly longer OS than patients with contrast-enhancing tumors distal from this region, regardless of methylation status (Fig. 5B; Log-rank, $p = 0.0025$). No difference in OS was detected between GBM patients having contrast-enhancing tumors on the left versus the right hemisphere (Fig. 5C, Log-rank, $p = 0.9601$), suggesting tumors that are localized to regions detected by ADIFFI analysis are different than simply separating patients by hemispheric involvement. Contrast-enhancing tumors that were localized to ADIFFI regions, combined with MGMT status, were able to further stratify patient survival (Fig. 5D), suggesting ADIFFI analysis may provide slightly more information than MGMT status alone. Cox proportional hazard analysis confirmed this observation, indicating KPS ($p < 0.0001$), MGMT methylation status ($p < 0.0001$), and tumors localized to the ADIFFI cluster ($p = 0.0069$) were independent prognostic factors. Median survival was 368 days longer for MGMT promoter methylated tumors localized to the left temporal lobe (median survival = 879 days) compared to unmethylated tumors localized elsewhere (median survival = 511 days).

Discussion

The current study examined the voxel-wise tumor frequency of occurrence in both T2/FLAIR hyperintense and contrast-enhancing regions in a total of 384 GBMs, representing the largest, most comprehensive pre-operative localization analysis of MGMT methylation status in human de novo GBM. Using a statistical mapping technique termed ADIFFI, which is similar in theory to the voxel-based lesion-symptom mapping (VLSM) technique (Bates et al., 2003), along with a permutation-based cluster-size correction (Bullmore et al., 1999), we have demonstrated a statistically significant number of MGMT promoter methylated tumors are localized to a distinct region of the left temporal lobe, and patients having tumors within this region have a statistical survival advantage, regardless of treatment.

Our findings suggest a substantial lateralization of MGMT promoter methylated tumors to the *left* temporal lobe region, and lateralization of MGMT unmethylated tumors to the *right* hemisphere, which has not been previously documented in human GBM. Asymmetry in human brain structure, function, and gene expression, in particular near the temporal lobe, is a well-documented phenomenon (Sun and Walsh, 2006) and may potentially explain this interesting observation. For example, anatomical differences have been observed between left and right hemispheres in the Sylvian fissures and the planum temporale (Rubens et al., 1976; Shapleske et al., 1999; Toga and Thompson, 2003). Paul Broca and Carl Wernicke documented lateralization of language function as early as the late 1800s (Broca, 1861; Wernicke, 1874). Additionally, structural and functional asymmetry has been documented in the motor cortex (e.g. handedness) (Amunts et al., 1996), as well as in many higher order functions (e.g. shape recognition, spatial attention, artistic skills, mathematical reasoning, etc.) (Borod et al., 2002; Gazzaniga, 2005). Differences in gene expression have also been documented between the two hemispheres (Sun et al., 2005), including many genes that have

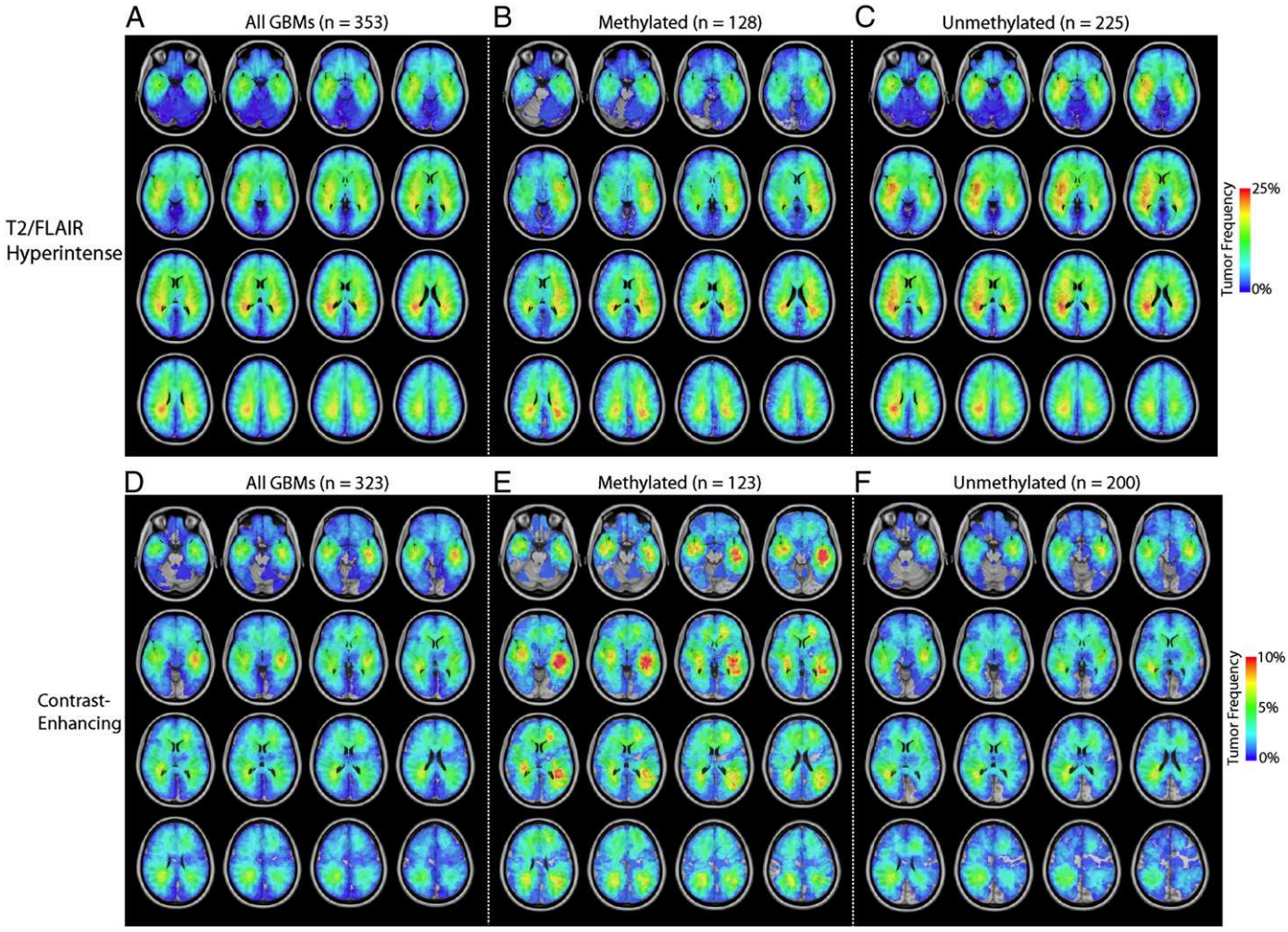

Fig. 3. Voxel-wise frequency of tumor occurrence for both T2/FLAIR hyperintense regions (A–C) and contrast-enhancing regions (D–F). A) T2/FLAIR hyperintense tumor frequency of occurrence for all GBM patients ($n = 379$). B) T2/FLAIR hyperintense tumor frequency of occurrence for MGMT promoter methylated patients ($n = 141$). C) T2/FLAIR hyperintense tumor frequency of occurrence for MGMT unmethylated patients ($n = 238$). D) Contrast-enhancing tumor frequency of occurrence for all GBMs ($n = 349$). E) Contrast-enhancing tumor frequency of occurrence for MGMT methylated tumors ($n = 136$). F) Contrast-enhancing tumor frequency of occurrence for MGMT unmethylated tumors ($n = 213$).

implications in human brain cancer. For example, the SUFU gene in the sonic hedgehog (SHH) pathway is over-expressed on the left hemisphere (Sun et al., 2005) and has been shown to be involved in regulation of brain tumor proliferation (Xu et al., 2008). This pathway has also been shown to regulate insulin-like growth factor-1 (IGF1) dependent malignant behaviors (Hsieh et al., 2011), is also over-expressed in the left hemisphere (Sun et al., 2005), and has also been shown to be involved in the control of cell proliferation (Ambrose et al., 1994). Similarly, many other genes demonstrate left-right hemisphere asymmetry and have been shown to play a role in tumorigenesis (Sun and Walsh, 2006), suggesting that lateralization of MGMT promoter methylation may be intimately involved with some of these pathways.

Another noteworthy observation in the current study was the relatively high frequency of occurrence of T2/FLAIR hyperintense regions near the posterior SVZ. This observation has been previously documented in a smaller number of patients (Alvarez-Buylla and Garcia-Verdugo, 2002; Barami et al., 2009); however, it may further support the cancer "stem-like" cell hypothesis (Nicolis, 2007; Sanai et al., 2005; Wechsler-Reya and Scott, 2001). Specifically, we observed T2/FLAIR hyperintensity in nearly 50% of de novo GBMs (approximately 25% on the right and 25% on the left hemisphere), suggesting roughly half of GBMs may originate from the posterior SVZ known to harbor neural stem cells. This region has long been proposed as a possible source of human gliomas (Globus and Kuhlenbeck, 1942). Animal exposure to carcinogens and cancer-causing viruses further support this theory, resulting in tumor formation within the SVZ (Copeland et al., 1975; Lantos and Cox, 1976; Vick et al., 1977) and quickly migrating into deep white matter regions, masking their ostensible source near the SVZ (Vick et al., 1977). Since neural stem cells have similar properties to glioma cells, including the ability to rapidly proliferate and migrate, it is possible that neural stem cells play a critical role in GBM formation. Alternatively, the observation of a relatively high frequency of occurrence of T2/FLAIR hyperintense regions may also have occurred due to these regions being especially prone to spreading of edema. The mechanism of peritumoral edema clearance into the cerebrospinal fluid is known to occur through the ventricles (Reulen, 2010), suggesting regions near the SVZ may also be a normal location of edema formation as it is transferred from tumoral regions, independent of the original site of tumor formation.

Interestingly, we observed a significant survival benefit for patients having tumors contiguous with the ADIFFI-classified cluster in the left

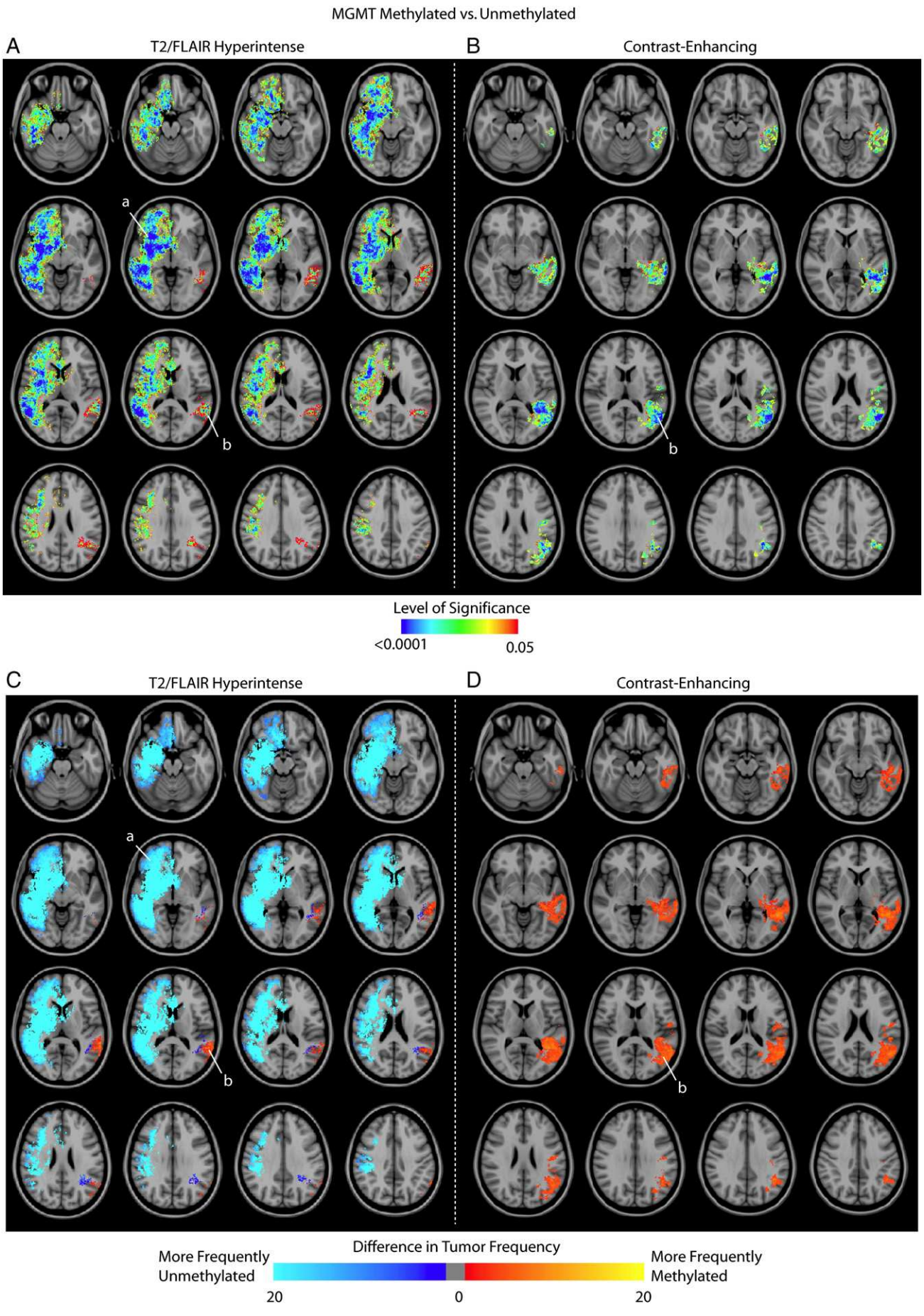
MGMT Methylated vs. Unmethylated
A
T2/FLAIR Hyperintense
B
Contrast-Enhancing
a
b
b
Level of Significance
<0.0001
0.05
C
T2/FLAIR Hyperintense
D
Contrast-Enhancing
a
b
b
Difference in Tumor Frequency
More Frequently Unmethylated
More Frequently Methylated
20
0
20

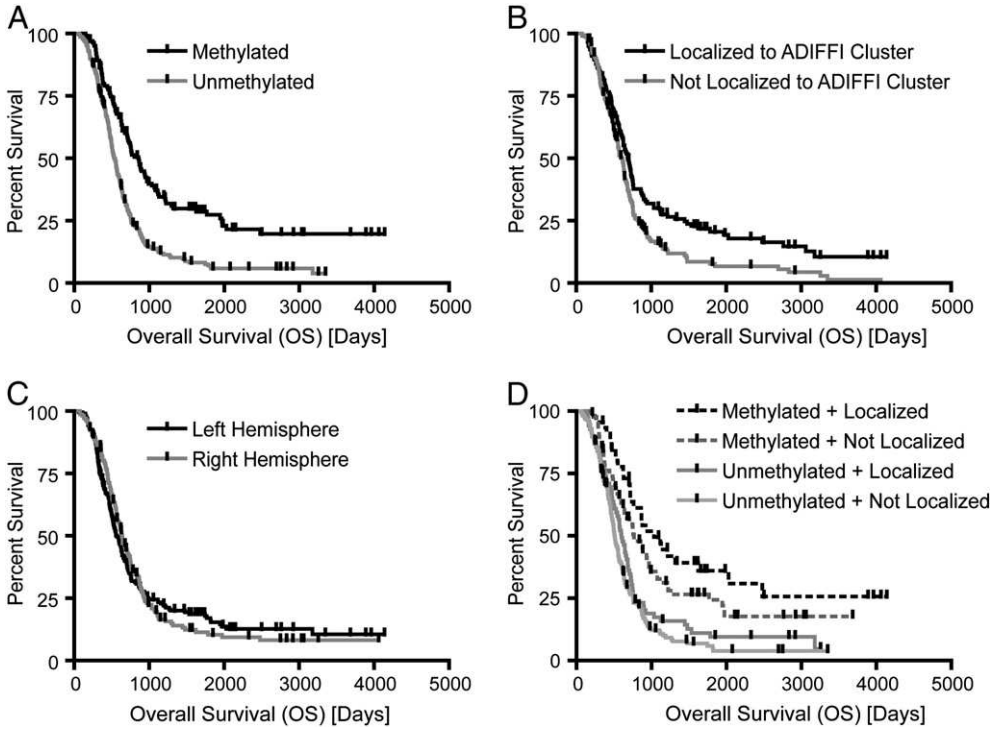

Fig. 5. Survival analyses for GBM patients. A) A statistically significant difference in overall survival (OS) from time of diagnosis was observed between MGMT promoter methylated and unmethylated tumors (Log-rank, $p < 0.0001$). B) A significant survival advantage (Log-rank, $p = 0.0049$) was observed in patients having contrast-enhancing tumors connected to the ADIFFI cluster, illustrated as "b" in Fig. 5B, compared to patients without enhacing tumor within this region, regardless of treatment or methylation status. C) No sigificant difference was observed between left and right hemispheric involvement (Log-rank, $p = 0.9601$), suggesting the effect shown in B) is isolated to the cluster in the left temporal lobe. D) Combining information about methylation status and tumor location allowed for further stratification of patient survival. Patients with MGMT promoter methylation *and* contrast-enhancing tumors localized near the ADIFFI cluster had a median survival advantage of 461 days compared to patients that were MGMT unmethylated *and* had contrast-enhancing tumors distal from the ADIFFI cluster (Cox Proportional Hazard Analysis; KPS, $p < 0.0001$; MGMT methylation status, $p < 0.0001$; tumor localized to ADIFFI cluster, $p = 0.0072$).

temporal lobe found to be associated with a high frequency of MGMT promoter methylation. Although this may appear to conflict with earlier reports demonstrating a significant survival advantage for patients with frontal lobe gliomas compared with other regions (Jeremic et al., 1994; Simpson et al., 1993), we did not specifically test whether there were survival differences between different generalized brain regions. Instead, we tested whether a survival difference existed between GBMs with contrast-enhancing lesions contiguous with a very specific region within the left temporal lobe and those located elsewhere in the brain (including but not limited to the frontal lobes). It is highly likely that tumors localized to other areas of the brain may also show survival differences, such as the frontal lobe regions where ADIFFI analysis has revealed the prognostically important IDH1 mutated tumors to be localized (Lai et al., in press).

Alternative approaches to the statistical analyses presented in the current study exist for the purposes of voxel-based lesion-symptom mapping (VLSM). For example, as an alternative to Fisher's exact test, investigators involved in studying ischemic stroke have chosen to implement Liebtermeister's quasi-exact method (Rorden et al., 2007), both because it is less conservative than Fisher's test and it is less computationally intensive. Additionally, some investigators have chosen to examine the distribution of maximum test statistic (t statistic, for example in (Kimberg et al., 2007)) during random permutations as an alternative to cluster-based correction. Future studies will focus on comparing these different techniques in the context of brain tumor localization.

In summary, we have demonstrated that human de novo GBMs occur in a high frequency within or contiguous with the posterior SVZ; that MGMT promoter methylated GBMs are preferentially lateralized to the left hemisphere, while MGMT unmethylated GBMs are lateralized to the right hemisphere; and that tumors near the left temporal lobe have a significantly longer overall survival compared with tumor occurring elsewhere, regardless of treatment or MGMT methylation status. Future studies will focus on validating these findings in a prospective, multicenter environment.

Supplementary materials related to this article can be found online at doi:10.1016/j.neuroimage.2011.09.076.

Acknowledgments

None.

Fig. 4. ADIFFI maps showing regional differences in statistical significance (p-value) and absolute difference in the number of MGMT methylated for the differences in tumor frequency between MGMT methylated and unmethylated tumors. A) ADIFFI results for T2/FLAIR hyperintense regions illustrating a large region on the right hemisphere (labeled "a") with low p-value along with a cluster on the left temporal lobe (labeled "b"). B) ADIFFI results for contrast-enhancing tumor regions illustrating similar cluster in left temporal lobe as in A). C) T2/FLAIR hyperintense tumor regions illustrate the large region on the right hemisphere (labeled "a") largely consists of MGMT unmethylated tumors, whereas the cluster in the left temporal lobe (labeled "b") consists of a larger number of MGMT promoter methylated tumors. D) Contrast-enhancing tumor regions also show localization of MGMT promoter methylated tumors in the left temporal lobe (also labeled "b").

References

Alvarez-Buylla, A., Garcia-Verdugo, J.M., 2002. Neurogenesis in adult subventricular zone. J. Neurosci. 22, 629–634.

Ambrose, D., Resnicoff, M., Coppola, D., Sell, C., Miura, M., Jameson, S., Baserga, R., Rubin, R., 1994. Growth regulation of human glioblastoma T98G cells by insulin-like growth factor-1 and its receptor. J. Cell. Physiol. 159, 92–100.

Amunts, K., Schlaug, G., Schleicher, A., Steinmetz, H., Dabringhaus, A., Roland, P.E., Zilles, K., 1996. Asymmetry in the human motor cortex and handedness. Neuroimage 4, 216–222.

Barami, K., Sloan, A.E., Rojiani, A., Schell, M.J., Staller, A., Brem, S., 2009. Relationship of gliomas to the ventricular walls. J. Clin. Neurosci. 16, 195–201.

Bates, E., Wilson, S.M., Saygin, A.P., Dick, F., Sereno, M.I., Knight, R.T., Dronkers, N.F., 2003. Voxel-based lesion-symptom mapping. Nat. Neurosci. 6, 448–450.

Borod, J.C., Bloom, R.L., Brickman, A.M., Nakhutina, L., Curko, E.A., 2002. Emotional processing deficits in individuals with unilateral brain damage. Appl. Neuropsychol. 9, 23–36.

Broca, P., 1861. Remarques sur le siège de la faculté du langage articulé, suives d'une observation d'aphémie (perte de la parole). Bull Soc Antropol 6, 330–357.

Bullmore, E.T., Suckling, J., Overmeyer, S., Rabe-Hesketh, S., Taylor, E., Brammer, M.J., 1999. Global, voxel, and cluster tests, by theory and permutation, for a difference between two groups of structural MR images of the brain. IEEE Trans. Med. Imaging 18, 32–42.

Copeland, D.D., Vogel, F.S., Bigner, D.D., 1975. The induction of intractranial neoplasms by the inoculation of avian sarcoma virus in perinatal and adult rats. J. Neuropathol. Exp. Neurol. 34, 340–358.

Cox, R.W., Jesmanowicz, A., 1999. Real-time 3D image registration for functional MRI. Magn. Reson. Med. 42, 1014–1018.

Drabycz, S., Roldan, G., de Robles, P., Adler, D., McIntyre, J.B., Magliocco, A.M., Cairncross, J.G., Mitchell, J.R., 2010. An analysis of image texture, tumor location, and MGMT promoter methylation in glioblastoma using magnetic resonance imaging. Neuroimage 49, 1398–1405.

Eoli, M., Menghi, F., Bruzzone, M.G., De Simone, T., Valletta, L., Pollo, B., Bissola, L., Silvani, A., Bianchessi, D., D'Incerti, L., Filippini, G., Broggi, G., Boiardi, A., Finocchiaro, G., 2007. Methylation of O6-methylguanine DNA methyltransferase and loss of heterozygosity on 19q and/or 17p are overlapping features of secondary glioblastomas with prolonged survival. Clin. Cancer Res. 13, 2606–2613.

Fontaine, D., Paquis, P., 2010. Glioblastoma: clinical, radiological and biological prognostic factors. Neurochirurgie 56, 467–476.

Gazzaniga, M.S., 2005. Forty-five years of split-brain research and still going strong. Nat. Rev. Neurosci. 6, 653–659.

Globus, J., Kuhlenbeck, H., 1942. Tumors of the stratothalamic and related regions: their probable source of origin and more common forms. Arch. Pathol. 24, 674–734.

Gorlia, T., van den Bent, M.J., Hegi, M.E., Mirimanoff, R.O., Weller, M., Cairncross, J.G., et al., 2008. Nomograms for predicting survival of patients with newly diagnosed glioblastoma: prognostic factor analysis of EORTC and NCIC trial 26981-22981/CE.3. Lancet Oncol. 9, 29–38.

Harpold, H.L., Alvord Jr., E.C., Swanson, K.R., 2007. The evolution of mathematical modeling of glioma proliferation and invasion. J. Neuropathol. Exp. Neurol. 66, 1–9.

Hegi, M.E., Diserens, A.C., Gorlia, T., Hamou, M.F., de Tribolet, N., Weller, M., et al., 2005. MGMT gene silencing and benefit from temozolomide in glioblastoma. N. Engl. J. Med. 352, 997–1003.

Hsieh, A., Ellsworth, R., Hsieh, D., 2011. Hedgehog/GLI1 regulates IGF dependent malignant behaviors in glioma stem cells. J. Cell. Physiol. 226, 1118–1127.

Jeremic, B., Grujicic, D., Antunovic, V., Djuric, L., Stojanovic, M., Shibamoto, Y., 1994. Influence of extent of surgery and tumor location on treatment outcome of patients with glioblastoma multiforme treated with combined modality approach. J. Neurooncol 21, 177–185.

Kimberg, D.Y., Coslett, H.B., Schwartz, M.F., 2007. Power in voxel-based lesion-symptom mapping. J. Cogn. Neurosci. 19, 1067–1080.

Lacroix, M., Abi-Said, D., Fourney, D.R., Gokaslan, Z.L., Shi, W., DeMonte, F., et al., 2001. A multivariate analysis of 416 patients with glioblastoma multiforme: prognosis, extent of resection, and survival. J. Neurosurg. 95, 190–198.

Lai, A., Tran, A., Nghiemphu, P.L., Pope, W.B., Solis, O.E., Selch, M., et al., 2010. Phase II study of bevacizumab plus temozolomide during and after radiation therapy for patients with newly diagnosed glioblastoma multiforme. J. Clin. Oncol. 29, 142–148.

Lai, A., Kharbanda, S., Tran, A., Solis, O., Pope, W., Pujara, K., Carrillo, J., Pandita, A., Peale, F., Ellingson, B.M., Bowers, C.W., Soriano, R.H., Mohan, S., Yong, W.H., Forrest, W.F., Seshagiri, S., Modrusan, Z., Aldape, K., Mischel, P., Liau, L., Escovedo, C., Chen, W., Nghiemphu, P., James, C.D., Prados, M., Westphal, M., Lamzsus, K., Cloughesy, T.F., Phillips, H., in press. Evidence for sequenced molecular evolution of IDH1 mutant glioblastoma from a distinct cell of origin. J Clin Oncol.

Lantos, P.L., Cox, D.J., 1976. The origin of experimental brain tumours: a sequential study. Experientia 32, 1467–1468.

Marino, S., Vooijs, M., van Der Gulden, H., Jonkers, J., Berns, A., 2000. Induction of medulloblastomas in p53-null mutant mice by somatic inactivation of Rb in the external granular layer cells of the cerebellum. Genes Dev. 14, 994–1004.

Nicolis, S.K., 2007. Cancer stem cells and "stemness" genes in neuro-oncology. Neurobiol. Dis. 25, 217–229.

Park, H.-J., Levitt, J., Shenton, M.E., Salisbury, D.F., Kubicki, M., Kikinis, R., et al., 2004. An MRI study of spatial probability brain map differences between first-episode schizophrenia and normal controls. Neuroimage 22, 1231–1246.

Pietsch, T., Waha, A., Koch, A., Kraus, J., Albrecht, S., Tonn, J., et al., 1997. Medulloblastomas of the desmoplastic variant carry mutations of the human homologue of *Drosophila* patched. Cancer Res. 57, 2085–2088.

Reulen, H.J., 2010. Bulk flow and diffusion revisited, and clinical applications. Acta Neurochir. Suppl. 106, 3–13.

Rorden, C., Karnath, H.O., Bonilha, L., 2007. Improving lesion-symptom mapping. J. Cogn. Neurosci. 19, 1081–1088.

Rubens, A.B., Mahowald, M.W., Hutton, J.T., 1976. Asymmetry of the lateral (sylvian) fissures in man. Neurology 26, 620–624.

Sanai, N., Alvarez-Buylla, A., Berger, M.S., 2005. Neural stem cells and the origin of gliomas. N. Engl. J. Med. 353, 811–822.

Shapleske, J., Rossell, S.L., Woodruff, P.W., David, A.S., 1999. The planum temporale: a systematic, quantitative review of its structural, functional and clinical significance. Brain Res. Brain Res. Rev. 29, 26–49.

Simpson, J.R., Horton, J., Scott, C., Curran, W.J., Rubin, P., Fischbach, J., et al., 1993. Influence of location and extent of surgical resection on survival of patients with glioblastoma multiforme: results of three consecutive Radiation Therapy Oncology Group (RTOG) clinical trials. Int. J. Radiat. Oncol. Biol. Phys. 26, 239–244.

Stupp, R., Mason, W.P., van den Bent, M.J., Weller, M., Fisher, B., Taphoorn, M.J., et al., 2005. Radiotherapy plus concomitant and adjuvent temozolomide for glioblastoma. N. Engl. J. Med. 352, 987–996.

Sun, T., Walsh, C.A., 2006. Molecular approaches to brain asymmetry and handedness. Nat. Rev. Neurosci. 7, 655–662.

Sun, T., Patoine, C., Abu-Khalil, A., Visvader, J., Sum, E., Cherry, T.J., et al., 2005. Early asymmetry of gene transcription in embryonic human left and right cerebral cortex. Science 308, 1794–1798.

Swanson, K.R., Bridge, C., Murray, J.D., Alvord Jr., E.C., 2003. Virtual and real brain tumors: using mathematical modeling to quantify glioma growth and invasion. J. Neurol. Sci. 216, 1–10.

Toga, A.W., Thompson, P.M., 2003. Mapping brain asymmetry. Nat. Rev. Neurosci. 4, 37–48.

Vick, N.A., Lin, M.J., Bigner, D.D., 1977. The role of the subependymal plate in glial tumorigenesis. Acta Neuropathol. 40, 63–71.

Wechsler-Reya, R., Scott, M.P., 2001. The developmental biology of brain tumors. Annu. Rev. Neurosci. 24, 385–428.

Wernicke, C., 1874. Der Aphasische Symptomenkomplex: Eine Psychologische Studie auf Anatomischer Basis. Cohn und Welgert, Breslau.

Xu, Q., Yuan, X., Liu, G., Black, K.L., Yu, J.S., 2008. Hedgehog signaling regulates brain tumor-initiating cell proliferation and portends shorter survival for patients with PTEN-coexpressing glioblastomas. Stem Cells 26, 3018–3026.

Zlatescu, M.C., TehraniYazdi, A., Sasaki, H., Megyesi, J.F., Betensky, R.A., Louis, D.N., Cairncross, J.G., 2001. Tumor location and growth pattern correlate with genetic signature in oligodendroglial neoplasms. Cancer Res. 61, 6713–6715.